James Webb Space Telescope Orbit Determination Analysis

Sungpil Yoon[1], Jose Rosales[2] and Karen Richon[3]
[1, 2]*a.i. solutions, Inc., 10001 Derekwood Lane, Lanham, MD 20706, 301-306-1756, sungpil.yoon@ai-solutions.com, jose.rosales@ai-solutions.com*
[3]*Code 595, NASA/Goddard Space Flight Center, Greenbelt, MD 20771, 301-286-8845, karen.v.richon@nasa.gov*

Abstract: *The James Webb Space Telescope (JWST) is designed to study and answer fundamental astrophysical questions from an orbit about the Sun-Earth/Moon L2 libration point, 1.5 million km away from Earth. This paper describes the results of an orbit determination (OD) analysis of the JWST mission emphasizing the challenges specific to this mission in various mission phases. Three mid-course correction (MCC) maneuvers during launch and early orbit phase and transfer orbit phase are required for the spacecraft to reach L2. These three MCC maneuvers are MCC-1a at Launch+12 hours, MCC-1b at L+2.5 days and MCC-2 at L+30 days. Accurate OD solutions are needed to support MCC maneuver planning. A preliminary analysis shows that OD performance with the given assumptions is adequate to support MCC maneuver planning. During the nominal science operations phase, the mission requires better than 2 cm/sec velocity estimation performance to support stationkeeping maneuver planning. The major challenge to accurate JWST OD during the nominal science phase results from the unusually large solar radiation pressure force acting on the huge sunshield. Other challenges are stationkeeping maneuvers at 21-day intervals to keep JWST in orbit around L2, frequent attitude reorientations to align the JWST telescope with its targets and frequent maneuvers to unload momentum accumulated in the reaction wheels. Monte Carlo analysis shows that the proposed OD approach can produce solutions that meet the mission requirements.*

Keywords: *James Webb Space Telescope, orbit determination, libration point orbit*

1. Introduction

The James Webb Space Telescope (JWST), which is a scientific successor of the Hubble Space Telescope and the Spitzer Space Telescope, is designed to study and answer fundamental astrophysical questions ranging from the formation of the universe to the origin of planetary systems. JWST is being developed by the National Aeronautics and Space Administration (NASA), the European Space Agency (ESA) and the Canadian Space Agency (CSA). The project is working towards an October, 2018 launch.

JWST will be placed in an orbit about the Sun-Earth/Moon (SEM) L2 libration point, which is located about 1.5 million km from Earth (four times the distance to the Moon) on the opposite side of the Sun from the Earth. The maximum distance from the Earth to the JWST orbit will be about 1.8 million km.

The updated orbit determination (OD) performance assessment for JWST has not been published since the original JWST navigation concept paper in 2003 [1]. This paper provides an updated assessment of the OD performance and discusses the methods applied for the different mission phases. Section 2 addresses the launch and early orbit phase (LEOP) and transfer orbit phase. Section 3 addresses the nominal science operations phase.

2. Launch and Early Orbit Phase (LEOP) and Transfer Orbit Phase

As part of the flight dynamics support for the JWST mission, an initial assessment of the OD performance during the LEOP and transfer orbit phase was completed using the covariance analysis method. The results presented here are considered preliminary. Further analysis based on more rigorous modeling will be performed in the future.

Orbit solutions during the LEOP and transfer orbit phase are required to support mid-course correction (MCC) maneuvers expected at Launch (L)+12 hours for MCC-1a, L+2.5 days for MCC-1b, and L+30 days for MCC-2. For MCC-1a, the OD performance is evaluated at L+12 hours, using the L+8 hours epoch as a data cut-off. For MCC-1b and MCC-2, the OD performance is evaluated at the maneuver time using an OD solution based on tracking data collected for 12 hours starting 1.5 days prior to the maneuver.

2.1 Performance Assessment Method

The main assets supporting JWST orbit determination are the Deep Space Network (DSN) 34 meter Beam Waveguide (BWG) antennas from Canberra, Madrid and Goldstone. Their antenna identification numbers are Deep Space Station (DSS)-34 (Canberra), DSS-54 (Madrid) and DSS-24 (Goldstone). These assets will provide S-band two-way range and range rate measurements using the JWST omni-directional antennas. During LEOP, the ranging campaign is expected to start 45 minutes after separation. Telemetry and command support will be provided by the Tracking and Data Relay Satellites (TDRS) and the ESA Malindi ground station during the LEOP, but no tracking data will be available from these assets.

The OD performance assessment method for these phases used FreeFlyer® software that simulated range and range rate measurements and processed simulated measurements using an Iterative Batch Least Squares estimator. The resulting solution was then propagated to the desired epoch and compared with the reference trajectory. The orbit propagators for reference trajectory propagation and in the batch filter used a Runge-Kutta 8(9) integrator and an EGM96, 4x4 geopotential model. The gravity force from the Sun and the Moon was included during the propagation.

For LEOP OD analysis that supports MCC-1a planning, the initial epoch was an epoch after separation from the launch vehicle and the initial states were obtained from the powered flight ephemeris provided by the launch vehicle manufacturer, Arianespace, in their 2010 release [2]. These initial states were based on the assumption that the launch epoch is October 1st, 2018 at 11:45 UTC. The initial state vector and its associated standard deviations are summarized in Table 2.1 (off-diagonal terms of the covariance matrix are not shown in this paper, but the actual computation took them into account.) All initial states were defined in Cartesian elements and the reference frame was Mean of J2000 Earth Equator.

For the transfer orbit phase OD analysis that supports MCC-1b and MCC-2, the initial states were obtained from the reference mission ephemeris file. The reference ephemeris file was generated by propagating the state from separation and simulating nominal MCC-1a and MCC-1b maneuvers. MCC-2 was not included in the reference ephemeris generation because the goal

was to assess the performance one day before it happens. Due to the lack of initial state covariance information, very large standard deviations and zero correlations between the states were assumed for the present analysis. This way, more weight was given to the measurements as opposed to the initial state. Table 2.2 summarizes the initial conditions used to estimate the navigation solution to support MCC-1b. Table 2.3 summarizes the same information for MCC-2.

Table 2.1 Initial conditions for OD to support MCC-1a

EPOCH (UTC)	State (km, km/s)	1-σ (km, km/s)
Oct 01 2018 12:13:51.557	X = -4173.087	σ_X = 58.725
	Y = -6944.925	σ_Y = 22.285
	Z = -538.178	σ_Z = 6.371
	VX = 5.523	σ_{VX} = 0.009
	VY = -8.120	σ_{VY} = 0.045
	VZ = -0.972	σ_{VZ} = 0.003

Table 2.2 Initial conditions for OD to support MCC-1b

EPOCH (UTC)	State (km, km/s)	1-σ (km, km/s)
Oct 02 2018 03:15:07.300	X = 158222.184	σ_X = 200
	Y = -35826.901	σ_Y = 200
	Z = -9272.235	σ_Z = 200
	VX = 2.048	σ_{VX} = 0.1
	VY = -0.001	σ_{VY} = 0.1
	VZ = -0.073	σ_{VZ} = 0.1

Table 2.3 Initial conditions for OD to support MCC-2

EPOCH (UTC)	State (km, km/s)	1-σ (km, km/s)
Oct 29 2018 11:45:07.300	X =1327098.182	σ_X = 200
	Y = 280369.000	σ_Y = 200
	Z = 9696.150	σ_Z = 200
	VX = 0.125	σ_{VX} = 0.1
	VY = 0.144	σ_{VY} = 0.1
	VZ = 0.046	σ_{VZ} = 0.1

The next step is simulating the range and range rate measurements. To simulate these measurements, the FreeFlyer® software was used, and the reference ephemeris file and a contact analysis file (described below) were used as inputs.

The contact analysis used for this analysis is a report consistent with the reference ephemeris and defines when there is contact with a particular tracking asset. This contact analysis takes into account the line-of-sight between the spacecraft and the asset, the spacecraft attitude, and the omni-directional antennas' physical location on the spacecraft and their fields of view. During LEOP, the first contact with a tracking asset was Canberra, followed by Madrid. However, there was no contact with Goldstone during the first eight hours. Also, the contact time intervals for Madrid and Canberra were not contiguous. More precisely, between launch and the first hour and

fifty minutes, and approximately during thirty minutes starting at five hours and twenty minutes after launch, there was no contact with the DSN assets. During the 12-hour tracking period before MCC-1b, Canberra and Goldstone were the two main tracking assets visible with a 13 minutes contact with Madrid at the beginning of the tracking period. During the 12-hour tracking period before MCC-2, Canberra and Madrid were the two main tracking assets visible and there was no Goldstone contact throughout the tracking period.

The measurement simulation process was based on a number of assumptions. It was assumed that the sampling rate for all assets was 60 seconds and that tracking was provided continuously during the contact time. Also, the simulated measurements were bias-free and no ionospheric effect was simulated. However, Gaussian noise was added to the simulated range and range rate measurements with a standard deviation that was consistent with the weekly tracking data assessment performed by the Goddard Space Flight Center (GSFC) Flight Dynamics Facility for each DSN asset. Table 2.4 lists the values used, which were based on the weekly report on April 22nd, 2013.

Table 2.4 DSN Measurement Standard Deviations

	DSN Antenna		
	Canberra DSS-34	Madrid DSS-54	Goldstone DSS-24
Range (m)	3.548	6.450	2.458
Range Rate (m/sec)	0.051	0.044	0.088

The simulated measurements were processed in an Iterative Batch Least Squares OD routine that was configured to estimate the OD solution at the desired epoch. The next section shows the results obtained by applying this method.

2.2 Results

Errors and the propagated standard deviation values for MCC-1a, MCC-1b and MCC-2 are shown in Tables 2.5 through 2.7. The standard deviations were obtained from propagating the batch navigation solution covariance to the epoch of interest. The errors were obtained by comparing the OD solutions with the reference ephemeris.

Table 2.5 Errors and standard deviations at L+12 hours to support MCC-1a

Parameter	Error	1-σ	Unit
X	-0.052	0.370	km
Y	-0.146	1.005	km
Z	-0.196	1.168	km
RSS Position	0.250	1.585	km
VX	-0.006	0.220	cm/sec
VY	-0.260	1.722	cm/sec
VZ	-0.288	1.497	cm/sec
RSS Velocity	0.388	2.292	cm/sec

Table 2.6 Errors and standard deviations at L+1.5 days to support MCC-1b

Parameter	Error	1-σ	Unit
X	0.024	0.138	km
Y	0.200	1.052	km
Z	-0.068	1.051	km
RSS Position	0.213	1.493	km
VX	2.910	0.097	cm/sec
VY	0.436	0.617	cm/sec
VZ	-0.130	0.618	cm/sec
RSS Velocity	2.945	0.879	cm/sec

Table 2.7 Errors and standard deviations and errors at L+29 days to support MCC-2

Parameter	Error	1-σ	Unit
X	-0.013	1.580	km
Y	0.035	7.279	km
Z	0.645	6.201	km
RSS Position	0.646	9.692	km
VX	0.009	1.234	cm/sec
VY	-0.057	5.720	cm/sec
VZ	0.410	4.108	cm/sec
RSS Velocity	0.414	7.150	cm/sec

The magnitude of the root sum squared (RSS) position standard deviation was on the order of 1 km for MCC-1a and MCC-1b and 9 km for MCC-2. The velocity standard deviation was about 2 cm/sec for MCC-1a, 1 cm/sec for MCC-1b and 7 cm/sec for MCC-2. In the future analysis, more attention will be paid to MCC-2, where the performance was significantly worse than the OD for MCC-1a and MCC-1b. As for the errors, in all three cases, the RSS differences from the reference ephemeris were less than 1 km in position and at the cm/sec level for velocity.

Mid-course correction analysis reported in [3] using these results shows that the OD performance values above are sufficient to support the MCC maneuver planning.

3. Orbit Determination Analysis for the Science Operations Phase

JWST will have a large sunshield with a maximum effective solar radiation pressure (SRP) area of ~163 m^2. The purpose of the sunshield is to protect the JWST optical system from infrared sources, including the Sun, Earth, and Moon and spacecraft bus electronics. The large SRP force acting on the huge sunshield poses the major challenge to accurate JWST OD during the nominal science operations phase, when JWST is orbiting Sun-Earth/Moon L2. Other challenges are frequent attitude reorientations to align the JWST telescope with its targets and frequent maneuvers to unload accumulated momentum in the reaction wheels.

For JWST mission, there is no position determination requirement for deterministic OD. Even though there are position prediction requirements, those will not be discussed in this paper. In

terms of the velocity determination requirement, the JWST maneuver planning team imposes 2 cm/sec velocity determination requirement to meet the mission lifetime goal of 10.5 years. A large velocity determination error at the time of stationkeeping (SK) maneuver design will result in a larger actual SK maneuver error, which will lead to more fuel consumption for SK and an overall shorter mission lifetime. The SK maneuver planning time is 24 hours before SK maneuver execution. The point of interest (POI) for velocity determination performance assessment is 2 hours earlier than the planning time, which is 26 hours before SK maneuver execution.

Orbit Determination Took Kit® (ODTK) version 6.2.0 [4] was used to simulate and process measurements. The extended Kalman filter (EKF) was chosen as a navigation filter over the least square batch estimation algorithm because of its capability to solve through the momentum unloading (MU) maneuvers and SK maneuvers as well as its capability to model the SRP coefficient as a varying quantity. Monte Carlo (MC) analysis method was used to assess the OD performance.

3.1 Reference Trajectory and Filter Setup

Fig. 3.1 (next page) shows the reference trajectory in rotating libration point (RLP) coordinate frame centered at SEM L2. This ephemeris was generated using a single trajectory from the SK analysis [5]. The initial epoch was March 20, 2019 12:00:00.000 UTC, which assumed to be after all commissioning activities, and the reference ephemeris duration was 14 months. The orbit box size was from -0.315×10^6 km to 0.150×10^6 km in the x-direction, from -0.730×10^6 km to 0.730×10^6 km in the y-direction and from -0.456×10^6 km to 0.355×10^6 km in the z-direction in the RLP frame.

Total of 19 SK were executed every 21 days with the first maneuver after about 40 days from the initial epoch. Table 3.1 lists the number of MU maneuvers (MU) between SK maneuvers. The magnitudes of SK maneuvers varied between 4.92 cm/sec and 15.89 cm/sec and the magnitudes of MU maneuvers varied between 0.22 cm/sec and 0.60 cm/sec. The ΔV information provided to the filter was deviated with 20% magnitude error and 5-degree direction error to simulate ΔV knowledge error during real operation. The deviated ΔV information was provided to the filter, and the filter was set to estimate maneuver ΔV corrections to compensate for the ΔV knowledge error.

The attitude profile of JWST was randomly generated with the following characteristics: Attitude changes at fixed intervals of 6 hours and orientation is uniformly distributed within the limits allowed by the mission to make sure that JWST instruments remain in the sunshield shade. Even though the ~~same~~ identical attitude profile was used in the filter ~~without error~~, the effect of the attitude knowledge error was simulated by deviating the solar radiation pressure model.

NASA GSFC's Solar Pressure and Aerodynamic Drag (SPAD) tool [5] was used to model the solar radiation pressure. SPAD is a ray tracing modeling tool for solar pressure and aerodynamics force and torque upon arbitrarily shaped objects in space. The SPAD model for JWST was validated against the SRP model provided by the spacecraft manufacturer, Northrop

Grumman Aerospace Systems. A SPAD plugin developed by NASA provides ODTK® with the SRP force corresponding to the JWST attitude. The SRP force computed by the plugin is a multiplication of a value from SPAD model with coefficient of solar radiation pressure (Cr).

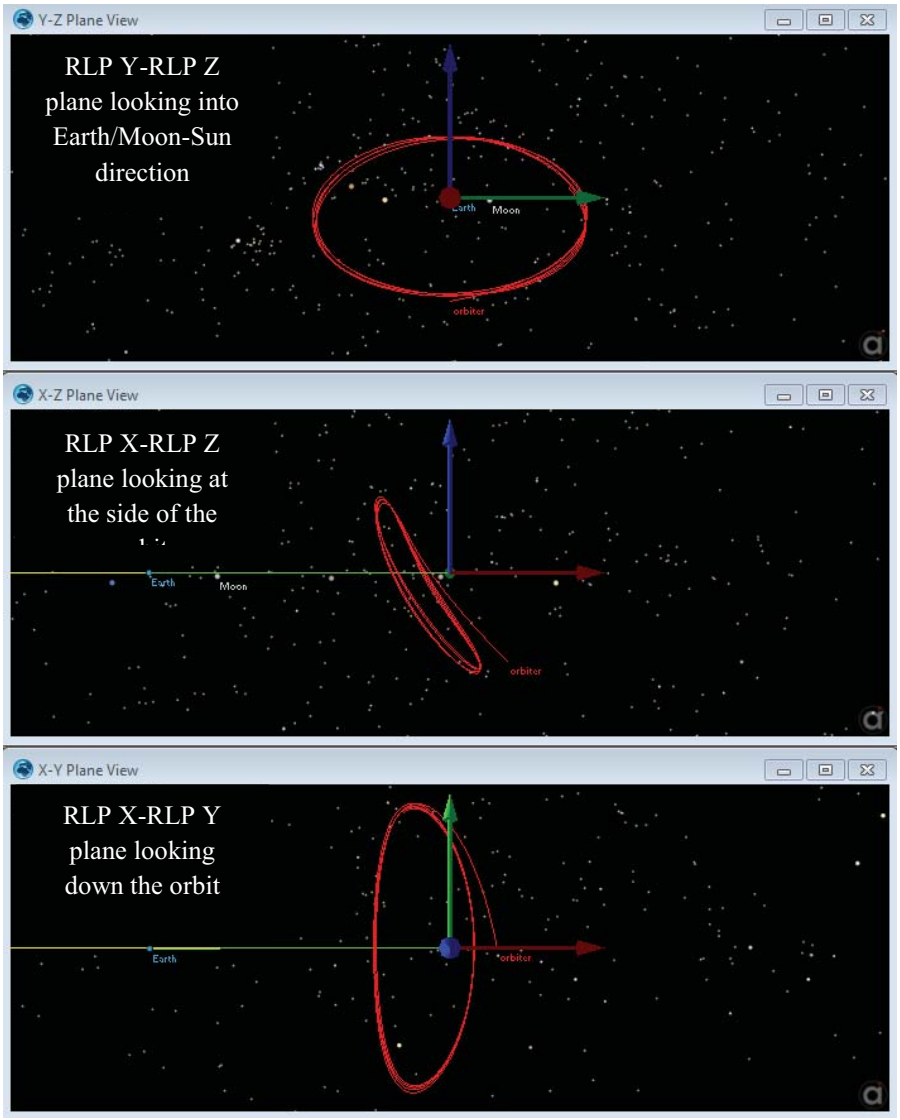

Figure 3.1 Reference trajectory in RLP frame (Yellow line is the SEM line)

Table 3.1 Number of MU maneuvers between the SK maneuvers

SK ID	1	2	3	4	5	6	7	8	9	10	11	12	13	14	15	16	17	18
# of MU	4	3	3	3	5	4	4	4	4	4	6	6	5	2	3	2	1	2

In the filtering process, correction of the Cr from nominal value was modeled as a second order Gauss-Markov stochastic process and estimated. In propagating the reference trajectory, the undeviated SPAD table was used while the SPAD table used in filter was deviated by a predefined noise to simulate error in SRP modeling. Two sets of noise, as summarized in Table

3.2, were injected into SPAD table to simulate the effect of SRP modeling error in magnitude and direction. This error simulates also the effect of attitude error. Table 3.3 lists the force model parameters used for reference trajectory propagation and in the navigation filter.

Table 3.2 Test cases

	SRP Model Error (1- σ)	Tracking Schedule
Case 1	1% magnitude and 1˚ direction error	Two 3-hour contacts
Case 2	1% magnitude and 1˚ direction error	Two 30-minute contacts
Case 3	5% magnitude and 5˚ direction error	Two 3-hour contacts
Case 4	5% magnitude and 5˚ direction error	Two 30-minute contacts

Table 3.3 Force model parameters

	Reference Trajectory	Filter
Third body	Sun, Moon	Sun, Moon
Geopotential field	EGM96, 21x21	EGM96, 8x8
Integrator	RK 7/8, variable step	RK 7/8, 5 min step
SK/MU maneuvers	truth	20% mag and 5˚ pointing error (1-σ)
SRP	Undeviated SPAD table	Deviated SPAD table (refer to Table 3.4)
Cr	Constant=1	Nominal(=1) + Second order Gauss Markov process with σ =1, half-life=360 minutes

3.2 Measurement Simulation and Filter Setup

The same ground tracking assets assumed in Section 2, namely the DSN 34 meter antennas at the Canberra, Goldstone and Madrid ground stations, were assumed as tracking facilities. According to the current tracking plan, there will be two tracking passes each day, one from Goldstone (Northern hemisphere) and the other from Madrid (Northern hemisphere). Every three days, Canberra tracking (Southern hemisphere) will replace one of the two daily passes. Tracking from both Northern and Southern hemispheres is important since the improved tracking geometry enables better OD performance. Table 3.2 (above) lists the tracking scenarios assumed in the current study. Cases 1 and 3 used 3-hour contacts for a total of 6 hours of daily tracking, and Cases 2 and 4 used 30-minute contacts for a total of 1 hour of daily tracking.

Range and range rate tracking data were simulated using ODTK®. It was assumed that the sampling rate for all assets is 60 seconds and that tracking is provided continuously during the contact time. Table 3.4 summarizes parameter values that were used to simulate instrument and environmental error effects on tracking data. Ionosphere effects were not simulated since the model data provided by ODTK® did not cover the year 2019 time period. It was assumed that transponder bias is calibrated through prelaunch testing. The residual transponder bias due to temperature variations was modeled in ODTK® as a second-order Gauss Markov process.

For each Monte Carlo run, the following parameters were varied randomly: initial states, transponder delay, measurement bias with white noise, troposphere bias, measurement time bias

and SPAD table error. The navigation filter was set to solve for the following parameters: three position components, three velocity components, Cr correction, MU and SK maneuver ΔV vectors, range and range rate biases.

Table 3.4 Measurement error model parameters

	Measurement Simulation	Filter
Troposphere	SCF model in ODTK®	Not modeled
Ionosphere	Not modeled	Not modeled
Estimate range bias	n/a	Yes
Range bias	1 m	0 m (initial)
Range bias σ	15 m	30 m
Range bias half life	1440 min	60 min
Range white noise σ	15 m	30 m
Estimate range-rate bias	n/a	Yes
Range-rate bias	0 cm/sec	0 cm/sec (initial)
Range-rate bias σ	0.1 cm/sec	0.2 cm/sec
Range-rate bias half life	1440 min	60 min
Range-rate white noise σ	0.1 cm/sec	0.2 cm/sec
Estimate transponder bias	n/a	No
Transponder bias	0 nanosec	n/a
Transponder bias σ	110 nanosec	n/a
Transponder bias half life	1440 min	n/a
Measurement time bias	Random walk with 1-σ = 0.001 sec	n/a

3.3 Results

A Monte Carlo simulation was run 30 times for each of four cases shown in Table 3.2. Figures 3.2 through 3.5 (on the next two pages) show filter performance as a function of time in radial, in-track and cross-track frame (RIC). The navigation filter makes the initial convergence by the time of the first SK maneuver, which happened about 40 days after the initial epoch.

The effect of SK maneuvers are clearly seen in these plots as the covariance increases at the time of maneuver execution in both position and velocity error plots although the covariance increase is more apparent in velocity error plots. Velocity errors in all three directions become large right after SK maneuvers as shown with large blue spikes, but converge within 20 days after SK maneuver execution, before the maneuver planning time for the next SK maneuver. There is no noticeable filter performance degradation at the times of MU maneuver execution showing that the navigation filter was effectively tuned to handle MU maneuvers.

It was noticed that position and velocity errors in April ~ May period (around 30 ~ 60 and 395 ~ 425 days in the figures) is bigger than errors in the other period. This pattern has one year frequency and more apparent in position error plots. Even though it was suspected that the spacecraft and the ground stations have disadvantageous geometry for OD in this season, the authors could not prove this hypothesis decisively. More investigation will be done on this topic

involving more than one reference ephemeris to test various geometry between the spacecraft and the ground stations.

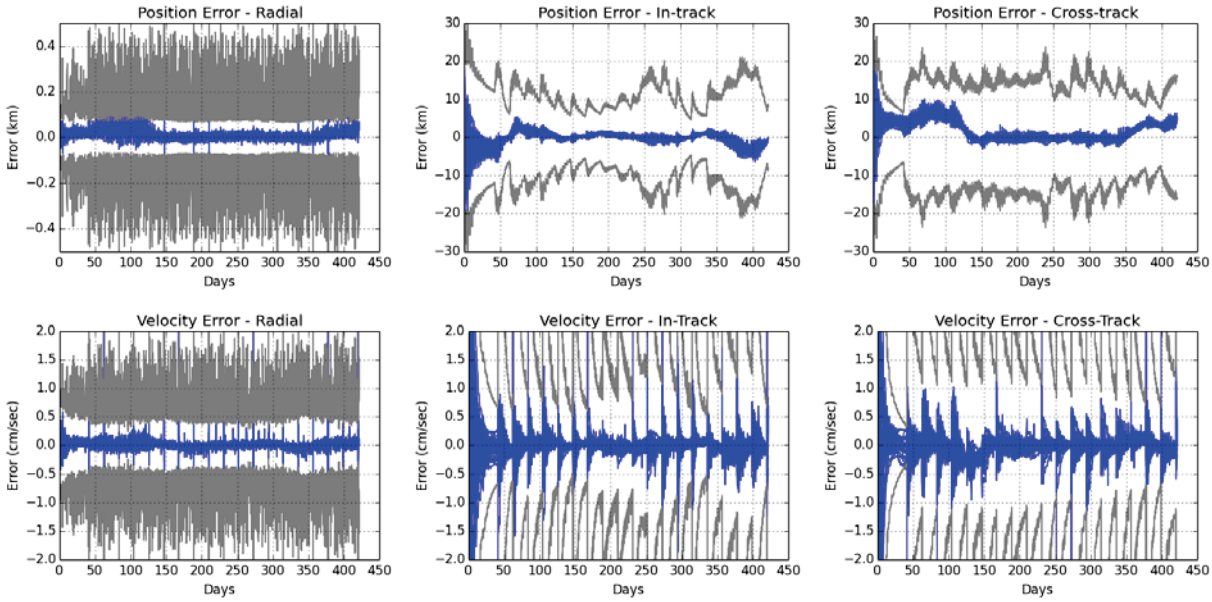

Figure 3.2 Position and velocity errors (blue) with ±3σ (gray) for Case 1 from all Monte Carlo runs

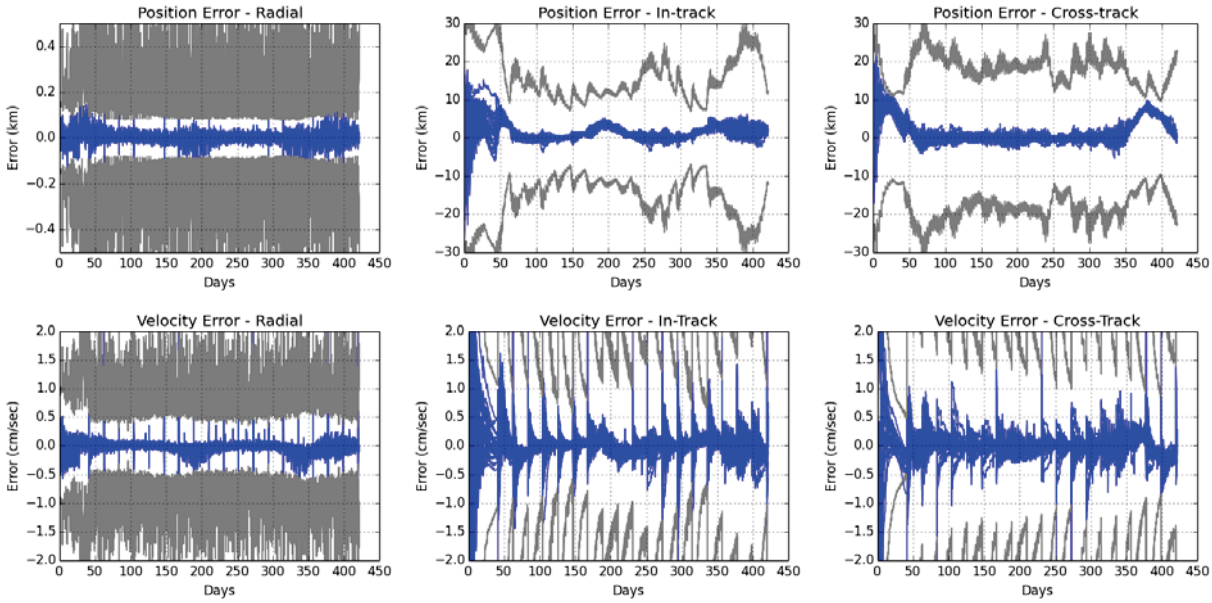

Figure 3.3 Position and velocity errors (blue) with ±3σ (gray) for Case 2 from all Monte Carlo runs

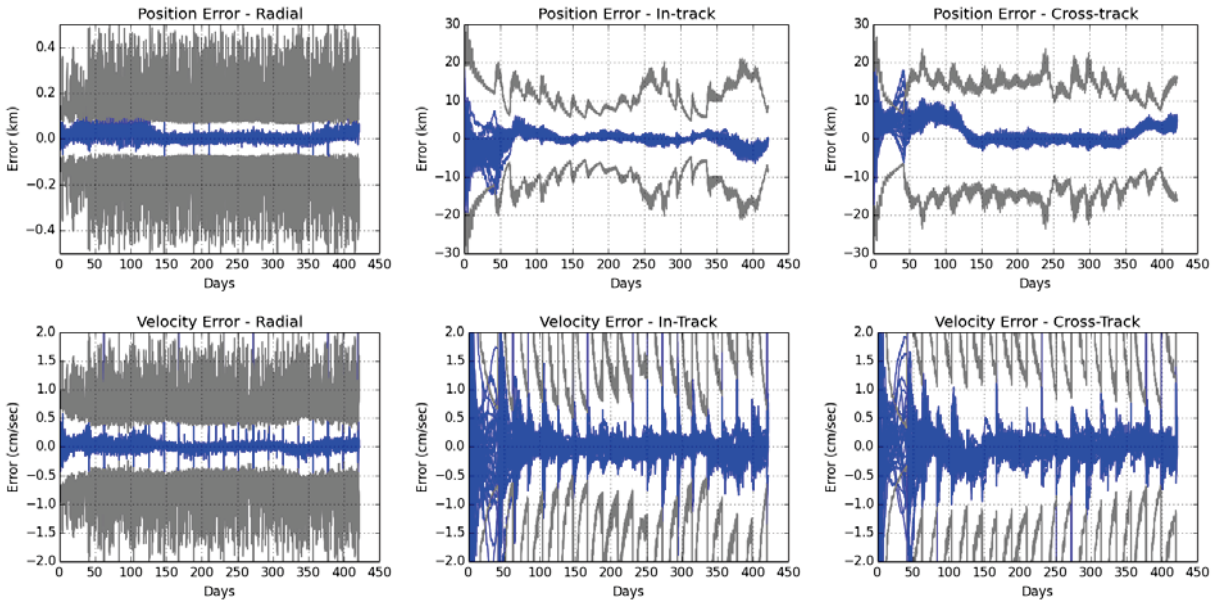

Figure 3.4 Position and velocity errors (blue) with ±3σ (gray) for Case 3 from all Monte Carlo runs

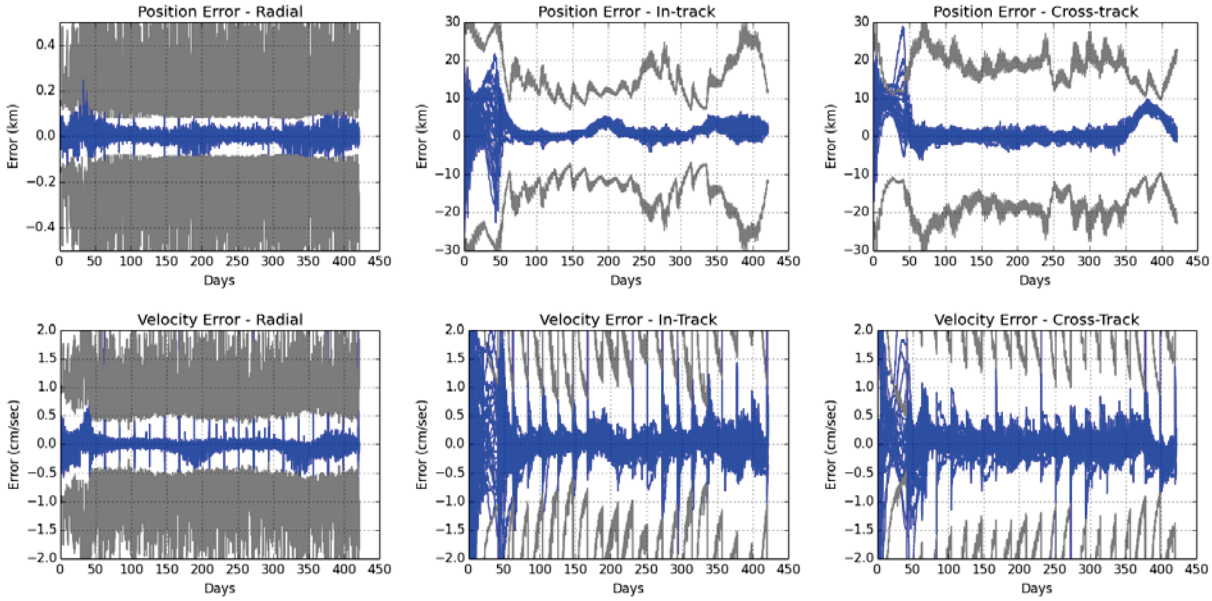

Figure 3.5 Position and velocity errors (blue) with ±3σ (gray) for Case 4 from all Monte Carlo runs

Figure 3.6 shows filter tuning quality in the estimation consistency plots. The quantities being plotted in these plots are errors normalized by state estimation uncertainty computed by the filter:

$$\text{estimation consistency} = \frac{error}{\sigma} \tag{1}$$

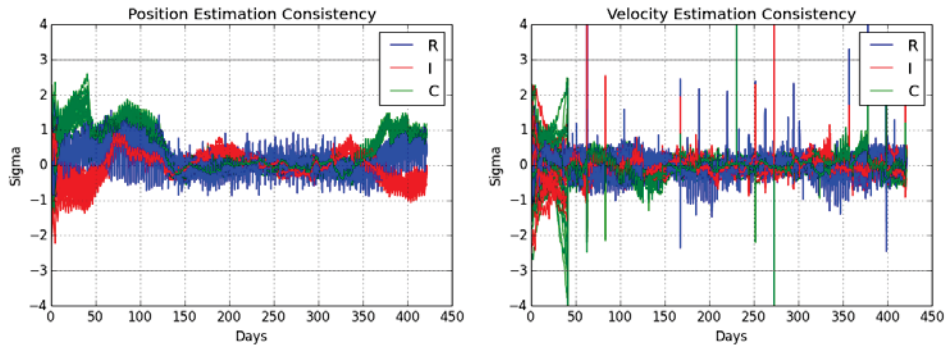

(a) Case 1

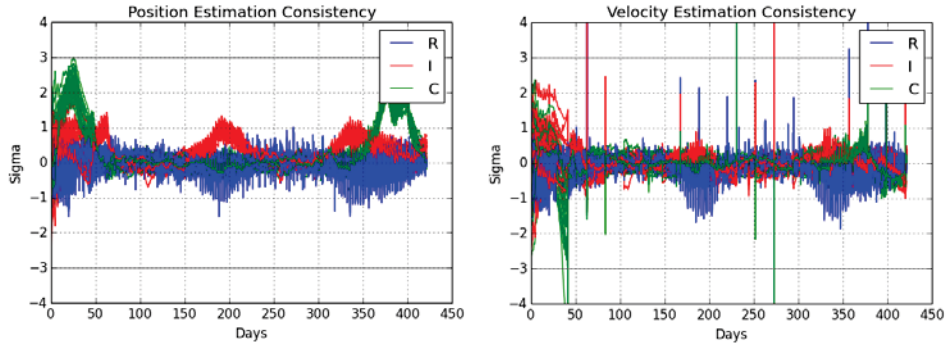

(b) Case 2

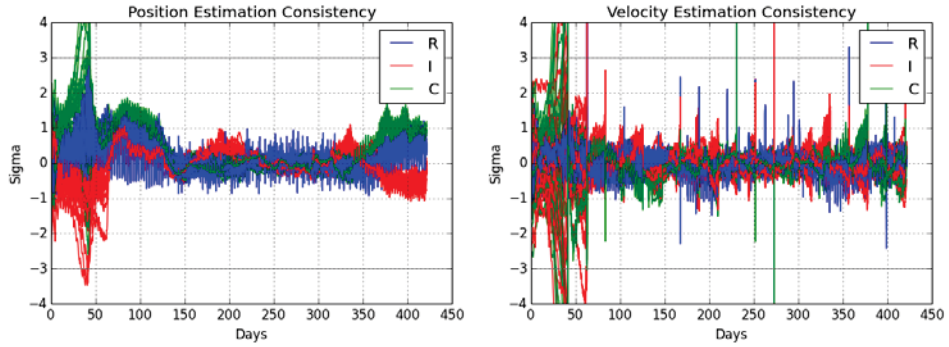

(c) Case 3

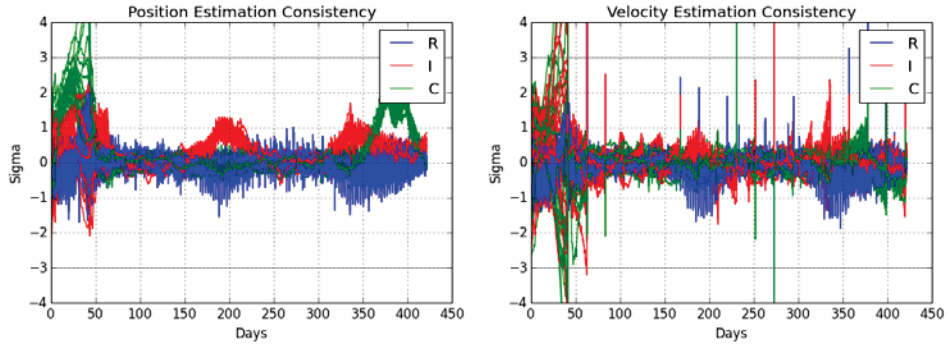

(d) Case 4

Figure 3.6 Position and velocity estimation consistency plots from all Monte Carlo runs

A consistency plot from a properly tuned navigation filter should have most (99.7%) of its data point within ±3 lines, which was the case as shown in Fig 3.6. Most of the peaks in the plots occur at the stationkeeping maneuver times.

Figure 3.7 shows estimated Cr correction values. Since the nominal Cr is 1 and this is the value used for reference trajectory propagation, the estimated Cr correction should be close to 0 without bias. In general, the estimated values shown in Figure 3.7 remain close to zero with no apparent bias. The initial convergence period can be seen in these plots, especially for case 4.

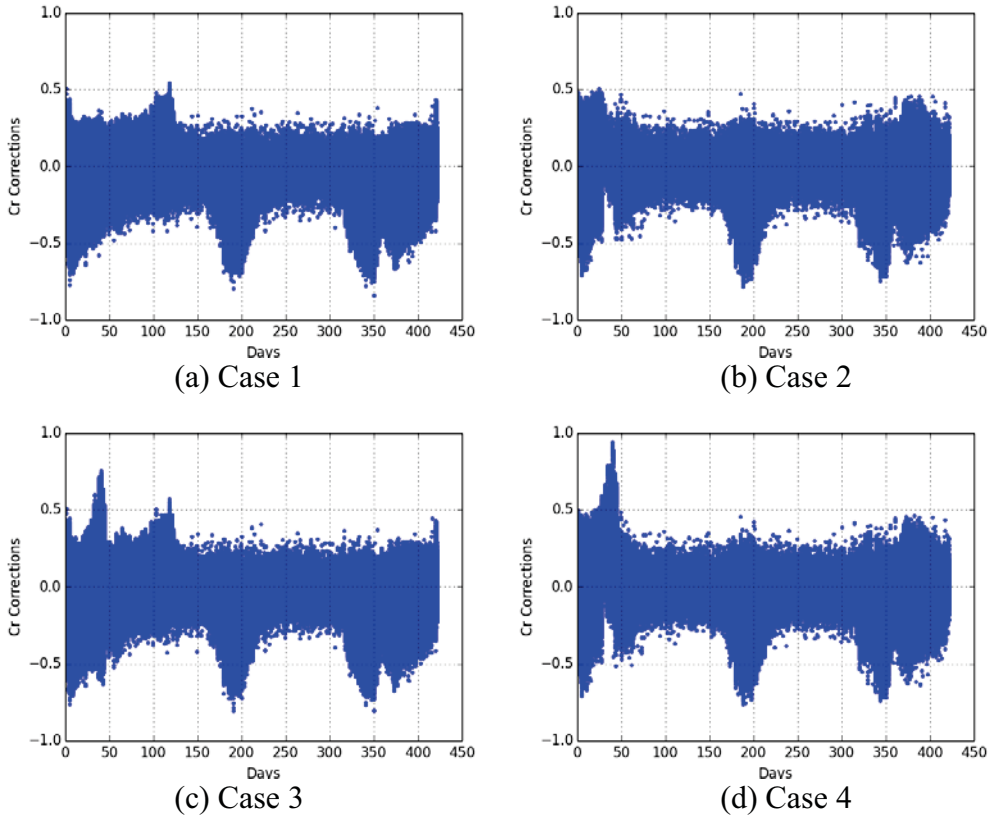

(a) Case 1 (b) Case 2

(c) Case 3 (d) Case 4

Figure 3.7 Estimated Cr corrections from all Monte Carlo runs

Table 3.5 summarizes measurement residual root mean square (RMS) values. In computing these RMS values, the initial convergence period (first 60 days) was excluded to make sure the numbers represent the filter performance in steady state. When 3-hour tracking contacts were assumed (Cases 1 and 3), the residual RMS is 15.71 m for range measurements and 0.10 cm/sec for range-rate measurements. These values are consistent with corresponding values used for measurement simulation, namely the measurement white noise sigma values shown in Table 3.4. When 30-minute tracking contacts were assumed (Cases 2 and 4), the residual RMS went up slightly, even though the magnitudes of increase were not big enough to cause concern.

Table 3.5 Measurement residual RMS from all Monte Carlo runs excluding initial convergence period (60 days)

	Range RMS (m)	Range-rate RMS (cm/sec)
Case 1	15.71	0.10
Case 2	17.07	0.11
Case 3	15.71	0.10
Case 4	17.09	0.11

To see if filter performance meets requirements, two different sets of statistics were computed. The first statistics (3x RMS) is defined as

$$3 \times \text{RMS} = 3\sqrt{(Error\ RMS_R)^2 + (Error\ RMS_I)^2 + (Error\ RMS_C)^2} \quad (2)$$

The second statistics (MAX) is defined as

$$\text{MAX} = \sqrt{(Error\ Max_R)^2 + (Error\ Max_I)^2 + (Error\ Max_C)^2} \quad (3)$$

Both of them are considered to be conservative measures to assess the filter performance of position and velocity estimation.

Both statistics were computed using results from all Monte Carlo cases and their values are listed in Tables 3.6 and 3.7. To assess the steady state performance, results for the first 60 days were excluded from the statistics computation. Based on both statistics, position estimation performance reaches about 10 km in all 4 cases. Variation of statistics values between cases is insignificant.

Table 3.6 Position estimation performance index (3x RMS) from all Monte Carlo runs excluding first 60 days (km)

	$3x\ RMS_{Radial}$	$3x\ RMS_{In\text{-}track}$	$3x\ RMS_{Crosstrack}$	3x RMS
Case 1	0.06	4.08	8.90	9.79
Case 2	0.06	5.31	7.12	8.88
Case 3	0.06	4.28	8.96	9.93
Case 4	0.06	5.50	7.25	9.10

Table 3.7 Position estimation performance index (MAX) from all Monte Carlo runs excluding first 60 days (km)

	MAX_{Radial}	$MAX_{In\text{-}track}$	$MAX_{Crosstrack}$	MAX
Case 1	0.27	6.39	10.10	11.95
Case 2	0.60	6.15	9.97	11.73
Case 3	0.27	6.44	10.74	12.53
Case 4	0.61	6.55	9.95	11.93

The POI for the velocity estimation performance assessment is 26 hour before the SK maneuver execution as mentioned previously. Since there are 19 SK maneuvers, there are 19 POI's for velocity estimation performance assessment. However, to assess the steady state performance, the first two POI's were excluded in the statistics computation. Tables 3.8 and 3.9 show that based on both statistics, velocity estimation performance meets the 2 cm/sec requirement with good margin in all 4 cases. Values for Cases 2 and 4 are larger than those for Cases 1 and 3, indicating that less tracking data results in degraded velocity estimation performance. Numbers for Case 3 and 4 are larger than those for Cases 1 and 2 indicating that larger SRP modeling error results in degraded velocity estimation performance.

Table 3.8 Velocity estimation performance index (3x RMS) from all Monte Carlo runs excluding first two POIs (cm/sec)

	$3x\ RMS_{Radial}$	$3x\ RMS_{In\text{-}track}$	$3x\ RMS_{Crosstrack}$	3x RMS
Case 1	0.12	0.23	0.29	0.39
Case 2	0.21	0.29	0.32	0.48
Case 3	0.12	0.40	0.41	0.59
Case 4	0.21	0.42	0.45	0.65

Table 3.9 Velocity estimation performance index (MAX) from all Monte Carlo runs excluding first two POIs (cm/sec)

	MAX_{Radial}	$MAX_{In\text{-}track}$	$MAX_{Crosstrack}$	MAX
Case 1	0.15	0.31	0.31	0.47
Case 2	0.19	0.32	0.35	0.51
Case 3	0.14	0.49	0.43	0.67
Case 4	0.21	0.53	0.54	0.78

4. Conclusions and Future Work

Based on the preliminary analysis presented in this paper, the OD accuracies expected during the LEOP and transfer orbit phase are adequate to support the MCC maneuvers. However, the presented analysis was based on several assumptions and simplifications. One of these assumptions that will be revisited in future analyses was that only DSN assets were used. However, other assets might be included in future analysis, such as TDRSS or a ground station at Malindi, Kenya. Adding these extra assets might provide a more accurate picture of what can be expected in terms of OD performance, especially during the critical period from injection to MCC-1a. Also, in terms of the measurement modeling, the presented analysis added only Gaussian noise to the range and range rate measurements. Future analysis will include a more rigorous modeling, including atmospheric errors, biases, and the spacecraft transponder delay. Note that for MCC-2 the Cr should be estimated since at that epoch the sunshield will have been deployed. This will be added in future analyses. Finally, contingency scenarios, such loss of a particular asset will be considered.

For the nominal science operations phase, the Monte Carlo analysis presented in this paper shows that position and velocity determination requirements will be met by making use of the sequential filter orbit determination approach. JWST preliminary OD analysis for this mission phase reported in [1] used different tools, different models and different assumptions. Therefore,

comparing results between those reported in the preliminary OD analysis with those reported in this paper is difficult. However, recalling the previous expectation of the JWST OD performance can give illumination on how to interpret the current results. JWST OD performance reported in [1] was: maximum position error = 4 km (1% SRP error), 17 km (5% SRP error), maximum velocity error = 0.3 cm/sec (1% SRP error), 0.6 cm/sec (5% SRP error). Current high fidelity results are consistent with those preliminary results. Other studies about OD performance of other L2 missions, such as WMAP, Planck and Gaia, consistently report about 10km or better position accuracy and better than 1 cm/sec velocity accuracy. [6, 7, 8] Based on the results reported in this paper, similar OD performance is achievable for JWST in spite of large sunshield and frequent MU maneuvers.

Future work includes 1) making use of more than one reference trajectories to represent different geometry between ground stations and spacecraft, 2) improving simulation fidelity such as solving for residual transponder bias in the filer and simulating ionospheric effect in simulating range and range rate measurements and 3) sensitivity analysis for contingency cases such as missing ground contacts and more dense momentum unloading maneuvers.

5. References

[1] Long, A, Leung, D., Kelbel, D., Beckman, M. and Gramling, C., "Navigation Concepts for the James Webb Space Telescope." Proceedings of the 2003 Flight Mechanics Symposium held at NASA Goddard Space Flight Center, NASA/CP-2003-212246, John. P. Lynch Editor, October 28-30, 2003.

[2] "Injection Accuracy Post Launch Vehicle TIM", Excel data from Arianespace through e-mail communication. November 2013.

[3] Petersen, J., Tichy, J., Wawrzyniak, G. and Richon, K., "James Webb Space Telescope Initial Mid-Course Correction Monte Carlo Implementation Using Task Parallelism." Proceedings 24th International Symposium on Space Flight Dynamics – 24th ISSFD, Laurel, MD, USA, 2014

[4] Hujsak, R., Woodburn, J. and Seago, J, "The Orbit Determination Tool Kit (ODTK), Version 5." AAS 07-125, AAS Astrodynamics Specialist Conference, Mackinac Island, MI, August 2007

[5] Dichmann, D., Alberding, C. and Yu, W., "Stationkeeping Monte Carlo Simulation for the James Webb Space Telescope." Proceedings 24th International Symposium on Space Flight Dynamics – 24th ISSFD, Laurel, MD, USA, 2014

[6] Truong, S., Cuevas, O. and Slojkowski, S., "Orbit Determination Support for the Microwave Anisotropy Probe (MAP)." Proceedings 13th AAS/AIAA Space Flight Mechanics Conference, Ponce, Puerto Rico, 2003

[7] Godard, B., Croon, M., Budnik, F. and Morley, T., "Orbit Determination of the Planck Satellite." Proceedings 21st International Symposium on Space Flight Dynamics – 21st ISSFD, Toulouse, France, 2009

[8] Budnik, F., Croon, M. and Morley, T., “Orbit Reconstruction for the Gaia Mission.” Proceedings 23rd International Symposium on Space Flight Dynamics – 23rd ISSFD, Pasadena, CA, USA, 2012